Journal Pre-proof

Detection of Phthalate Esters in PET bottled Drinks and Lake water using Esterase/ PANI/CNT/CuNP based Electrochemical Biosensor

Jayshree Annamalai, Namasivayam Vasudevan

PII: S0003-2670(20)30974-0

DOI: https://doi.org/10.1016/j.aca.2020.09.041

Reference: ACA 237980

To appear in: *Analytica Chimica Acta*

Received Date: 10 August 2020

Revised Date: 21 September 2020

Accepted Date: 22 September 2020

Please cite this article as: J. Annamalai, N. Vasudevan, Detection of Phthalate Esters in PET bottled Drinks and Lake water using Esterase/PANI/CNT/CuNP based Electrochemical Biosensor, *Analytica Chimica Acta*, https://doi.org/10.1016/j.aca.2020.09.041.

Credit Author Statement

Jayshree Annamalai: Conceptualization, Methodology, Investigation, Writing- Orginal draft preparation, Software, Formal analysis. **Namasivayam Vasudevan:** Supervision, Writing-Review and Editing, Validation.

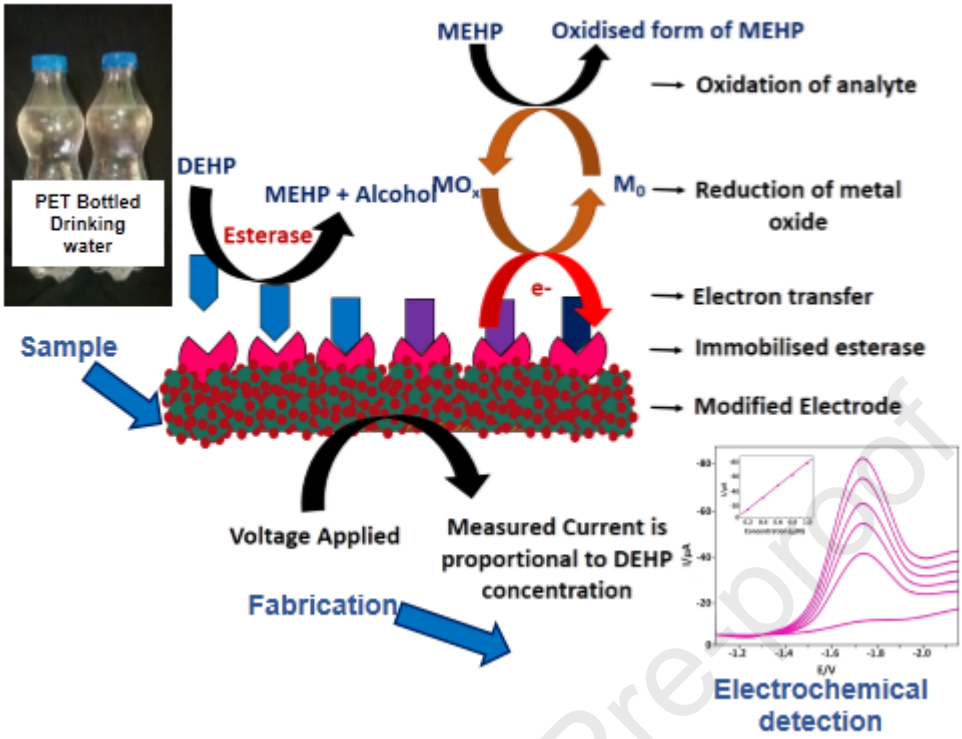

Detection of Phthalate Esters in PET bottled Drinks and Lake water using Esterase/PANI/CNT/CuNP based Electrochemical Biosensor

Jayshree Annamalai* and Namasivayam Vasudevan
Centre for Environmental Studies, Department of Civil Engineering,
Anna University, CEG Campus, Chennai- 600025, India
*Corresponding author e-mail: jayshreeannamalai@yahoo.com

Detection of Phthalate Esters in PET bottled Drinks and Lake water using Esterase/PANI/CNT/CuNP based Electrochemical Biosensor

Abstract

Phthalate esters (PEs) are the most common plasticizers that tends to exhibit endocrine disruption. Since, these PEs are used in the manufacture of PET bottles and PVC products: point of exposure magnifies up on consumption of PET bottle and plastic container stored drinking water and beverages. Apart from human exposure to PEs, bioaccumulation of PEs and toxic effects among wildlife also seems to be divergent. In the present study, an enzyme-based biosensor for the detection of PEs was developed to overcome the tedious extraction procedures involving PE extraction and sophisticated instruments for the detection. Linear Sweep voltammetry analysis of Nafion (NF) surface modified glassy carbon electrode with esterase (EST) and nano-components was carried-out. Peak potential of individual PEs were in the range of -1.72 to -1.82 V at the concentration of 1x 10^{-5} mmol L^{-1}. Sensitivity of EST/PANI/CNT/CuNP-NF modified GCE was determined in terms of detection limit and was calibrated to be 0.03-0.08 nmol L^{-1}. Thus, the developed enzyme based electrochemical sensor could be successfully employed in determining PE exposure in humans and bioaccumulation among aquatic flora and fauna via., consumption of PET bottle stored drinks and industrial effluents discharged into the lakes.

Keywords: esterase; phthalate esters; electrochemical biosensor; drinking water; lake water

1. Introduction

Among the known endocrine disruptors the most ubiquitous are the esters of 1-2-benzenedicarboxylic acid commonly known as phthalate esters. Ortho-phthalate diesters are commonly produced by alcoholic esterification of phthalic anhydride and di (2-ethylhexyl) phthalate (DEHP) constitutes more than 80% of the total phthalate production all over the world [1]. It had been suggested that DEHP pose highest toxicity and endocrine disruptive threat to human race, especially to the young children, infants, pregnant and nursing mothers [2]. Number of recent researches have suggested declining trend in the reproductive hormonal levels, damage to sperm DNA and count in male adults; whereas, elevated risk of altered breast development, breast cancer, premature puberty and prostate changes in females [3]. Among wildlife, phthalate esters (PEs) tends to cause immunotoxicity, neurotoxicity and endocrine disruption with an extended reports on reproductive disorders [4]. Since, PEs are not covalently bound to the poly vinyl chloride (PVC plastic) molecular structure- they leach, migrate, and evaporate directly into foodstuffs and atmosphere exposing human beings to PEs via., ingestion, inhalation and dermal routes [5].

Leaching of phthalates into food from packaging, from PET (PETE, polyethylene terephthalate) bottles into beverages and mineral water, and from corks of glass bottles has been reported. Phthalates leaching into orange juice from tetra packaging were 110 times above the safe intake limit of 6.0 μg/L set by US EPA (United States Environmental Protection Agency) during its shelf life and until close to its expiry date [6]. A maximum admissible concentration (MAC) of 3 μg L^{-1} for DEHP in water is established by the U.S. Environmental Protection

Agency (EPA) [7]. DEHP is the most widely used PE and it encompasses a quarter of the total production of plasticizers. Maximum PE concentration in the water samples of Asan Lake of Korea was reported to be 2.29 µg L^{-1} with bioaccumulation of 1081 µg Kg^{-1} dw^{-1} in fish [8]. The guideline for safe drinking water given by World Health Organization (WHO) and European Union (EU) in their water policy is set to be 8.0 µg L^{-1} DEHP as safe limit in fresh and drinking waters, according to list of priority compounds posing endocrine disrupting hazards to human [9].

Mostly, the extraction and pre-concentration steps are performed in advance to analyze trace levels of PEs in water samples, conventional methods include solid-phase extraction and liquid-liquid extraction [10, 11]. Contemporary analytical techniques used to measure phthalate concentrations in food products and beverages, such as gas chromatography/mass spectroscopy (GC/MS), require expensive and complicated instruments, trained professionals and laboratory environment with stringent conditions over sampling procedures [12, 13]. In the recent years, though researches involving the electrochemical and quartz crystal microbalance analysis of PEs have been reported, requirement to develop a reliable and highly sensitive quantification system remains an urging issue [14,15,16]. This development may provide on-site real-time detection and measurement of phthalates in beverages, food products, medicines and environmental samples; in turn dictating the paramount importance and urgency at present [17]. Thus, this is the first report on an enzyme based biosensor for the detection of phthalate esters in drinks stored in PET bottles and lake water contaminated with industrial effluents. In the present study, phthalate specific esterase (EST) enzyme was used in presence of nano-composite materials and linear sweep voltammetry (LSV) was performed.

2. Materials and methods

2.1. Chemicals and reagents

Styrene, aniline, di (2-ethylhexyl) phthalate (DEHP), diethyl phthalate (DEP), dimethyl phthalate (DMP), dibutyl phthalate (DBP), butyl-benzyl phthalate (BBP), Acetylene and Nafion (NF) were purchased from Sigma Aldrich. Electrolyte salts: tetramethyl ammonium bromide (TMAB), tetrabutyl ammonium bromide (TBAB), tetrabutyl ammonium perchorate (TBAP) and lithium perchlorate ($LiClO_4$), and other chemicals used in the experiments were of analytical grade. Stock solution of PEs (DEHP, DEP, DMP, DBP, BBP) and supporting electrolytes (TMAB, TBAB, TBAP, $LiClO_4$) were prepared at the concentration of 0.1 and 1.0 mol L^{-1} using chloroform; while working standards were prepared by diluting in distilled water. Potassium phosphate buffer solution was prepared using 0.2 M KOH and 0.2 M KH_2PO_4 at appropriate quantities. NaOH and HCl solutions each at the concentration of 1.0 mol L^{-1} were prepared individually using distilled water and used for adjusting pH. Esterase (EST) enzyme used for the detection of PEs was isolated from a bacterial strain, *Rhodococcus jostii* PEVJ9 capable of hydrolyzing micro-pollutant, DEHP [18]. Characterization of enzyme has also been carried-out in our previous study [19].

2.3. Instrumentation

In the study various instruments and apparatuses were used for the characterization of nanocomposite materials and analysis of electrochemical activities. Initially SEM analysis was carried-out using SEM, HITACHI S4L00 and was operated at 10 kV; EDAX analysis using

HORIBA instruments. Bruker Tensor 27 IR FTIR spectrometer was used identify the functional groups in the range from 500 to 4000 cm^{-1}. XRD analysis was performed using Xpert-Pro-PAN Analytical Instrument, using CuKα radiation (λ=1.540598 Å). Diffraction patterns were recorded in 2θ range of 10° to 80°. The identification of phases was made by referring to the Joint Committee on Powder Diffraction Standards International Center for Diffraction Data (JCPDS-ICDD) database using corresponding Powder Diffraction Files (PDF). XPS analysis was performed using Shimadzu ESCA 3100 instrument. The peaks were deconvoluted by means of a standard CasaXPS software (v.2.3.13; product of CasaXPS Software Ltd., U.S.A.) to resolve the separate constituents after background subtraction. Electrochemical measurements were performed using PGSTAT-12 electrochemical Analyser (AUTOLAB, The Netherlands BV) which constitutes a standard three electrode cell containing modified glassy carbon electrode as working electrode, Pt wire as auxillary electrode and Ag/AgCl as reference electrode.

2.4. Preparation of carbon nanotube and polymer based nanocomposite material

In the preparation of nanocomposite material, initially polystyrene (PS) sulfonated core particles were prepared by dispersing PS particles in 30 mL of concentrated sulphuric acid. Mono-dispersed PS particles were obtained by reacting 10 g of styrene with 10 mL of aqueous initiator containing 0.23 g of $(NH_4)_2S_2O_8$ under nitrogen atmosphere [20]. The sulfonation reaction was held for 4 h at 40 °C, then the product was collected by centrifuging and washing with distilled water [21]. The obtained wet PS/sulfonated core particles were made to react with distilled aniline monomer followed by addition of oxidant $(NH_4)_2S_2O_8$ and the reaction was held for 12 h. The end product was centrifuged, washed with distilled water and ethanol, and dried in vacuum at 40 °C for 24 h. Later, the dried PANI-coated PS core/shell particles were dispersed in

tetrahydrofuran to dissolve PS cores [21]. The resulting PANI hollow spheres were washed with distilled water and dried.

Synthesis of multiwalled carbon nanotubes (MWCNTs) was carried-out by chemical vapour deposition (CVD) method according to Muataz et al. [22]. In brief, acetylene (C_2H_2, 99.5% purity) was used as a hydrocarbon source, cobalt nanoparticles as catalyst, hydrogen as carrier gas and argon for flushing the air from the system. The reaction temperature ranged from 500 °C to 1200 °C, reaction time was about 45 min and hydrogen flow rate was 300 mL min^{-1}. Obtained CNTs were functionalized in presence of concentrated nitric acid (HNO_3). Copper nanoparticles were synthesized by chemical reduction method; where copper acetate was reduced in presence of organic acid and an amine derivative at room temperature (37 °C) [23]. To these prepared MWCNTs and CuNPs, the above prepared PANI hollow spheres were added and suspended in distilled water at the concentration of 1.0 mg mL^{-1}, and stirred continuously for 12 h at room temperature (37 °C) [24]. During reaction, CuNPs and CNTs gets into the PANI hollow spheres and adsorbs onto the surface of PANI leading to the formation of PANI/CNT/CuNP composite hollow spheres.

2.5. Preparation of EST blended modified glassy carbon electrode

Glassy carbon electrode (GCE) of 3 mm in diameter was initially polished with 1.0, 0.3, and 0.05 μm alumina slurry successively, rinsed with double distilled water and dried at room temperature. This was followed by ultrasonication of PANI/CNTs/Cu NPs nanocomposite, dispersed in distilled water at the concentration of 2.0 mg mL^{-1} of solution for 30 min. The resultant colloidal solution (5.0 μL) was then dropped onto the pretreated electrode surface and allowed to dry at room temperature for 2 h [24]. Then, 100 μL of EST (5 mg mL^{-1}) and 50 μL

NF (Dupont 5% wt) were ultrasonicated for 30 min and 5.0 μL of the suspension was subsequently casted onto the PANI/CNTs/CuNPs nanocomposite modified GCE and allowed to dry at 4°C for 2 h after each drop-casting step. Later, the enzyme and nanocomposite modified GCE was stored at 4°C and electrochemical studies were performed.

2.6. Characterization of the nanocomposite materials

The above prepared PANI hollow spheres, MWCNTs, CuNPs and PANI/CNTs/CuNPs nanocomposite materials were characterized using scanning electron microscopy (SEM) to understand the morphology, assembly and dimensions. Energy dispersive X-ray analysis was carried-out to identify and quantify elemental composition in the nanocomposite materials. Fourier transmission infrared (FTIR) spectroscopic analysis was performed to determine the other organic and inorganic groups involved in the interaction and formation of nanocomposite material. X-ray diffraction (XRD) spectroscopic analysis was performed to analyse the crystallinity of nanomaterials. X-ray photoelectron spectroscopy (XPS) was performed to analyse the composition of nanocomposite materials by measuring the energy of electrons. Cyclic voltammetric (CV) analysis was performed to measure current developed in an electrochemical cell in response to nanocomposite materials and electrochemical impedance spectroscopy (EIS) to analyse the impedance of system in dependence to AC potential frequency.

2.5. Linear Sweep Voltammetry analysis

Electrochemical measurements were performed at room temperature, 37±1 °C. Under optimized conditions, 10 mL of aqueous solution containing $1x10^{-5}$ mmol L^{-1} DEHP and 0.1 mol L^{-1} TBAB as supporting electrolyte at pH 7.0±0.1 was taken in the electrochemical cell (refer supplementary information). After applying all optimized parameters, LS voltammograms were

recorded in the range of -1.2 V to -2.2 V, scan rate at 0.9 V s^{-1}, stirring rate of 1400 rpm and deposition time of 20 s without nitrogen purging [25]. Blank solution was also scanned under similar conditions. LSV of varied electrode components: PANI, PANI/CNT, PANI/CNT/CuNPs, EST-PANI/CNT/CuNPs and commercial EST enzyme-PANI/CNT/CuNPs onto NF modified GCE were assessed against 1x 10^{-5} mmol L^{-1} of DEHP. Peak current and peak potential of DEHP at varied concentration ranging between (0-25) x 10^{-5} mmol L^{-1} was also calculated. The peak potential for the DEHP working standard was determined to be ~-1.72 V. Calibration plots were obtained for PEs: DEHP, DMP, DEP, DBP and BBP standard solutions (refer supplementary information). Concentration of PEs in spiked and real samples were calculated from specific calibration plot.

2.6. Analysis of PET bottle stored drinks and lake water

For the experimental analysis: drinking water, soft drinks and beverage PET bottles were purchased from local supermarket and stored at ambient temperature. Lake water samples were collected from different sites of Ambattur Lake, Chennai, Tamil Nadu, India (13.1000º N, 80.1400º E). Ambattur Lake is a rain-fed reservoir surrounded by State Industries Promotion Corporation of Tamil Nadu Limited (SIPCOT). Each of the stored PET bottle drink and lake water samples were pre-treated before analysis and were analyzed in six triplicates. The peak potentials were calculated for the concentration of PE based on the calibration linear curves and spiked standard accuracy. PEs recoveries were calculated by standard quantification from spiked preparation before and after evaporation depending on the determined validation elements. The obtained values were compared with that of retention values of GC-MS (refer supplementary information).

3. Results and Discussion

3.1. Characterization of nano-composite material

3.1.1. SEM analysis

PANI/CNT/CuNP composite was synthesized using sulfonated PS core shells as templates. Initially, conductive PANI polymer was synthesized in the presence of oxidant such that it covered the PS core shells as a layer, the thickness of which depends on the concentration of aniline and oxidant added to the reaction medium. Exposure to THF dissolute PS core shell leaving PANI spheres hollow (Fig. 1a). To these PANI hollow spheres, CNTs and CuNPs are adsorbed; amount of adsorption depends on the concentration of CNTs and CuNPs added to the reaction mixture and period of time constantly stirred (Fig. 1b, c) and Figure 1d reveals the adsorbed nano-components forming PANI/CNT/CuNP nanocomposite material along with EST enzyme [21]. EDAX pattern revealed the surface morphology of the nanocomposite material that has been deposited with carbon, nitrogen, oxygen and copper as major elements constituting about 27.54, 9.34, 27.33 and 16.83 % of weight (Fig. 1e). Thus, polymer, CNTs and CuNPs are key source for these elements; other than that magnesium, sodium, potassium, calcium and iron were present in trace concentration ranging between 0.52- 4.27 % of weight.

3.1.2. FTIR analysis

FTIR analysis of PANI/CNT/CuNP nanocomposite material had a stretch at 3642 cm^{-1} revealing the N-H stretching at 3201 and 2643^{-1} (Fig. 2a). A characteristic stretch at 1736 cm^{-1} indicated carboxylic group of nitric acid treated f-CNT and oxidation of carbon atoms present on the surface of CNTs [26] (Fig. 2b). Apart from these bands, C=O and C=C stretching vibrations at 1623 and 1521 cm^{-1} correspond to quinoid (Q) and benzenoid (B) ring which are characteristic of conducting PANI polymer. C-N stretching band at 1381cm^{-1} attributed to secondary aromatic amines and displacement of π electrons induced by acid doping of the polymers was observed [27]. FTIR spectrum analysis of the synthesized CuNPs have revealed the significant transmission peak at 623 cm^{-1} which is attributed to Cu (I)-O vibrations (Fig. 2c). Thus, FTIR spectrum of nano-composite material- PANI/CNT/CuNP reveals characteristic bands and stretches of nanomaterial and doped polymer used (Fig. 2d).

3.1.3. XRD analysis

XRD analysis of the PANI/CNT/CuNP nanocomposite revealed the complete blend of polymer, f-CNTs and CuNP. The peaks corresponding to PANI were observed at 21.26 and 29.82° 2θ with (100) and (211) as planes. The intensity of these peaks in nanocomposite material were found to be reduced which might be due to adsorption of CNT and CuNPs onto the surface of PANI; this behaviour also suggests reduction of crystalline property of the polymer [28, 29]. The diffraction peak at 26.5° corresponds to the f-CNT, in this case also reduction in intensity of peak was observed. Nano-composite had typical peaks of Cu nanoparticles at 43.31° and 50.45° that attributed to (111) and (200) planes; while, the planes (220) and (311) at 61.53 and 73.68° corresponded to Cu_2O nanoparticles. Thus, the nanocomposite peaks revealed the presence of characteristic peaks and planes related to nanomaterials and polymer, respectively (Fig.3).

3.1.4. XPS analysis

The survey scan spectrum of nanocomposite material: PANI/CNT/CuNP has revealed the presence of carbon, nitrogen, oxygen and copper elements. Presence of carbon (C1s) peak at ~285.2 eV was speculated mainly due CNTs. Nitrogen (N1s) peak ~400.1 eV rooted purely from the PANI polymer used for the preparation of nanocomposite. Oxygen (O1s) peak at ~532.2 eV was assured to be due to HCOOH used in the functionalization of CNTs and presence of Cu_2O. Finally, presence of copper ($Cu2p_{3/2}$ and $_{1/2}$) peak at ~934.0 eV corresponds to the copper nanoparticles used in nanocomposite material preparation (Fig. 4a). Carbon deconvoluted spectra revealed peaks at 284.2, 285.7 and 287.0 eV corresponding to C-C or C-H, C-N^+ or C=N^+ and C-O/C=O group. The characteristic peak of polymer at 284.0 eV and that of f-CNT 285.4 eV reveals presence emeraldine form the PANI and f-CNTs in nanocomposite material. The intensity of 284.0 eV peak was found to be reduced in PANI/CNT/CuNP material; this might be due to interaction between PANI and CNTs/CuNPs (Fig. 4b). Nitrogen (N1s) spectrum of PANI/CNT/CuNP had four distinct deconvoluted curves at 398.9, 399.1, 400.1 and 400.8 eV corresponding to different forms of nitrogen (Fig. 4c). Peak at 398.9 eV corresponds to pyrindine –N (=N-) form of nitrogen [31]. Peak at 399.1 eV might be due interaction between -N- group and CNT/CuNP and the pyrrolic-N peak was assumed from the peak at 400.1 eV [31, 32]. There was raise in the intensity of the peak at 400.8 eV that corresponded to the high binding energy of –N^+, suggesting interaction between N+ and protons introduced by acid dopants [33].

The deconvoluted oxygen (O1s) peaks were observed at 531.0, 532.1 and 533.0 eV associated with single and double bonds between oxygen and carbon and attributed to O=C, O-C and C-OH groups (Fig. 4d). There was reduction in intensity of 531.0 eV peak compared to that of deconvoluted peaks of CuNP and f-CNTs. This peak attributes to the hydroxyl oxygen

attached to carbon atoms, the reduction of this peak in the present study could be due adsorption of nanomaterials and polymer upon each other to form composite. While an increase in 532.1 eV peak attributes to adsorbed oxygen and lattice oxygen present as moisture which might be due blended form of nanomaterials [34]. The deconvoluted peaks for copper ($Cu2p_{3/2}$ and $Cu2p_{1/2}$) were at 933.6, 936.4, 953.7 and 956.2 eV (Fig. 4e). Compared to pure CuNP to that of CuNPs in the nano-composite material had reduced peak intensity. Reduction in intensity might be due to interaction with other composite materials. Thus, on correlating increase, decrease, displacement and raise of new peaks suggested a well-bound interaction between nanocomposite materials yielding desired PANI/CNT/CuNP matrix for the immobilization of EST enzyme.

3.2. CV and EIS analysis

CV analysis of five different surface modified electrodes in presence of EST enzyme, PANI, CNT and CuNPs onto NF modified GCE was assessed. The modified electrodes were EST-NF modified GCE, EST/PANI-NF modified GCE, EST/PANI/CNT-NF modified GCE, EST/PANI/CNT/CuNP-NF modified GCE and a commercial EST enzyme modified PANI/CNT/CuNP-NF modified GCE for comparison with that of purified EST isolated from the DEHP degrading bacterial strain *Rhodococcus jostii* PEVJ9 [18]. Figure 5a illustrates a gradual increase in anodic and cathodic peak with the addition of PANI, CNTs and CuNPs. CNTs tends to have catalytically active surface which increases the active surface area of a modified electrode. In addition to this, when CuNPs were dispersed on the surface of EST/PANI/CNT-NF modified GCE, the peak current greatly increased [35]. In the present study, it is important to note that EST enzyme also has significant role in contributing diffusion of ferricyanide towards electrode surface.

In the case of EIS, Nyquist plot of impedance spectra is represented by a semicircle portion at higher frequencies corresponding to electron transfer limited process, while linear portion at lower frequencies corresponds to the diffusion process. Electron transfer resistance (R_{ct}) at the electrode surface is equal to the semicircle diameter describing the interface properties of the electrode [36]. In the present study, diameter of the semicircle gradually increased with the addition of PANI, CNTs and CuNPs (Fig. 5b). The R_{ct} of EST-NF modified GCE, EST/PANI- NF modified GCE, EST/PANI/CNT-NF modified GCE, EST/PANI/CNT/CuNP-NF modified GCE and a commercial EST enzyme modified PANI/CNT/CuNP-NF modified GCE were ~500, 2500, 3200, 5600, 3000 Ω, respectively. These increased rates of R_{ct} indicates the efficiency of electron transfer rate induced by nanocomponents. EST/PANI/CNT/CuNP-NF modified electrode with higher 5600 Ω indicates that purified EST molecules are well adsorbed to nanocomposite matrix as insulating layer on the electrode surface; rather commercial esterase [37].

3.3. Linear sweep voltammetric analysis

Electrochemical response of various components of NF modified electrode towards 1x 10^{-5} mmol L^{-1} DEHP were measured at optimal parameters. A consequential increase in peak current was found in the following order: PANI-NF modified GCE <PANI/CNT-NF modified GCE <PANI/CNT/CuNP-NF modified GCE <Commercial EST enzyme/PANI/CNT/CuNP-NF modified GCE <EST/ PANI/CNT/CuNP-NF modified GCE. Peak potential of the electrode components also varied with the addition of electrode components, the peak potential shifted towards lesser negative potential (Fig. 6a). Shift in peak potential was from -2.0 V to -1.9 V when CNTs were added to PANI-NF modified GCE, then to -1.72 V after the addition of CuNPs; this shows strong interaction between nanocomposite materials. While, no change in

peak potential after immobilization of EST enzyme onto nanomatrix suggested that enzyme does not interfere in electro-activity; in turn, nanocomposite materials improved electron transfer and surface area for adsorption [38]. CNTs and CuNPs tends to improve sensitivity and catalytic electroactive surface area by providing biocompatible environment to maintain the activity of enzyme; however, intensity of peak current increased in presence of enzyme [36]. Upon comparing peak current of purified EST enzyme (-100 µA) with that of commercial EST enzyme (-80 µA) was higher, this revealed the specificity of enzyme towards analyte (PE). Nanocomposite material coated with purified EST enzyme revealed an excellent electron transfer and increased peak current. This indicated surface-controlled process and further, average surface coverage of EST onto modified electrode was derived to be 1.4 x 10^{-9} mol cm^{-2} from Faraday's law (refer supplementary information).

LSV analysis was carried out at optimized parameters at varied concentration of (0-25) x 10^{-5} mmol L^{-1} DEHP using purified EST enzyme immobilized onto nanomaterial: PANI/CNT/CuNP-NF modified GCE. Single peak current was observed at each concentration with varied intensities ranging between -20 and -125 µA; the intensity increased as the concentration of DEHP increased (refer supplementary information). PEs have highly negative reduction potential and the peak potentials were investigated between -1.57- 1.8 V; while, in present study the peak potential was at -1.72 V [14, 15]. The R^2 of DEHP calibration curve was 0.998. Thus, the LSV results clearly reveals the linear transfer of electrons and excellent hydrolysis of DEHP to MEHP and phthalic acid as reported in our previous study [18]. Saeed et al. reported electrochemical analysis of water soluble PEs such a DEP, DMP, DBP and DPP (dipropyl phthalate) [25]. However, high molecular weight PEs: DEHP, DOP, DCHP and DiNP (di-iso nonyl phthalate) which are either sparingly soluble or insoluble in water did not show any

increase peak current. Contrastingly, in the present study DEHP showed gradual increase in peak current with the increase in concentration of DEHP. This action might be influenced by specific purified EST enzyme used in the study for the hydrolysis of PEs which in turn had improved electrochemical response.

LSV of the EST/PANI/CNT/CuNP-NF modified GCE in response to varied PEs: DEHP, DEP, DMP, DBP and BBP each at the concentration of 1x 10^{-5} mmol L^{-1} were studied. Results revealed slight variation among peak currents and peak potentials of five different PEs. Peak potential of ~-1.78, -1.72, -1.82, -1.77 and -1.82 V were determined in response to DEHP, DEP, DMP, DBP and BBP; while peak current were observed to be -87.9, -76.2, -90.1, -84.6 and -110.9 µA (Fig. 6b). Such less significant variation in peak current and potential provides a significant platform to determine PEs in mixtures. Qureshi et al. determined peak current and potential of DEP, DBP and DDP using hanging mercury drop minielectrode and reported the peak potentials and current to range between -1.6 and -1.7 V, and ~80.0- 110.0 µA [14]. These results were in agreement with the present study illustrating enzyme has no significant effect on electroactivity of modified electrodes; instead paved way in electrochemical determination of high molecular weight PEs.

3.4. Limit of detection and quantification

The statistical parameters of the calibration curves such as slope, intercept, correlation coefficient, limit of detection (LoD) and limit of quantification (LoQ) were calculated using statistic software OriginPro 7.5 (Table 1). R^2 for DEHP, DEP, DMP, DBP and BBP at the concentration (2-10) x 10^{-7} mmol L^{-1} were 0.995, 0.998, 0.993, 0.995 and 0.999. LoD and LoQ for DEHP (0.06 and 0.2 nmol L^{-1}), DEP (0.08 and 0.2 nmol L^{-1}), DMP (0.03 and 0.1 nmol L^{-1}),

DBP (0.04 and 0.1 nmol L^{-1}) and BBP (0.04 and 0.1 nmol L^{-1}) at 2-10 x 10^{-7} mmol L^{-1} were determined. RSD for intra-day and inter-day precision were 0-3.2 % and 0.1-2.9 % (Table 2). Accuracy of intra-day precision ranged 96-100%; while for inter-day precision were between 96-100% (refer supplementary information).

3.5. Detection of PEs in PET bottle stored drinks and lake water

LSV analysis of real samples revealed concentration of PEs in PET bottle stored drinking water, soft drinks and beverage, and lake water samples. Drinking water stored for 2, 4 and 6 months were found to have 0.240±0.001, 0.379±0.001, 0.522±0.001 µmol L^{-1}; soft drink samples stored for 1 and 3 months to be 4.109±0.006 and 12.654±0.045 µmol L^{-1}; beverage samples to be 0.226±0.015 and 1.824±0.010 µmol L^{-1}; and industrial effluent contaminated lake water samples to be 3.146 ± 0.003 µmol L-1. These electrochemically determined results were in agreement GC-MS analysis (refer supplementary information). The detection limits of PEs determined in the present study were also compared with that of reported electrochemical methods in PE detection (Table 3). This comparison reveals the efficiency of EST and nanocomposite material based NF modified GCE in detecting PEs (DEHP, DMP, DEP, DBP and BBP) most commonly present in PET bottle stored drinking water, soft drinks and beverages [19]. LoD (0.03-0.08 nmol L^{-1}) for PEs in the present study reveals its efficiency in determining PE contamination as per US EPA, WHO and EU standards [6, 9]. Since, shelf-life of an enzymatic biosensor is related to the loss of enzyme activity over time, shelf-life of EST/PANI/CNT/CuNP-NF modified GCE was determined. No changes in CV curves were observed at optimized parameters up to ~100 cyclic scans and retained its 96% activity for 40 d, when stored at 4°C.

4. Conclusion

This is the first report on enzyme based electrochemical biosensor for the detection of phthalate esters which is commonly termed as an 'endocrine disruptor'. In our day-to-day life, it has become essential to be aware of the micro-pollutants to which we are exposed and to be precautious on being exposed. Present study involving the detection of PEs in drinking water, soft drinks, beverages and lake water samples is an initiation to determine PE contamination in our consumables and environmental samples. However, further development and optimization is essential to carry-out PE analysis in more food and environmental samples. This would ensure bio-monitoring, risk assessment and safety management of PEs; concerned to analyzing viable exposure and toxic effect causing concentration among humans and wildlife in a simple, cost-effective and reliable manner.

5. Acknowledgement

This research was supported by University Grants Commission (UGC), New Delhi, India and we thank the UGC for their gesture by endowing Basic Science Research Fellowship.

6. References

1. Z.R. Gallinger, G.C. Nguyen, Presence of phthalates in gastrointestinal medications: Is there a hidden danger? World J. Gastroenterol. 19(2013) 7042-7047.

2. E. Ripamonti, E. Allifranchini, S. Todeschi, E. Bocchietto. Endocrine disruption by mixtures in topical consumer products. Cosmetics. 5(2018) 61.

3. T.H. Yen, D.T. Lin-Tan, J.L. Lin. Food safety involving ingestion of foods and beverages prepared with phthalate-plasticizer-containing clouding agents. J. Formos. Med. Assoc. 110(2011) 671-684.

4. C.R. Tyler, A. Parsons, N.J. Rogers, A. Lange, A.R. Brown, Plastics and their impact on wildlife, in: R.M. Harrison R.E. Hester (Eds.), Plastics and the Environment, RSC publishers, 2019, pp. 106-130.

5. J. Annamalai, V. Namasivayam, Endocrine disrupting chemicals in the Atmosphere: Their effects on Humans and Wildlife. Environ. Int. 76(2015) 78-97.

6. N. Rastkari, M. Zare Jeddi, M. Yunesian, R. Ahmadkhaniha, The effect of storage time, temperature and type of packaging on the release of phthalate esters into packed ccidic liquids. Food Technol Biotechnol. 55(2017) 562–569.

7. P. Prapatpong, W. Kanchanamayoon, Determination of Phthalate Esters in Drinking Water using Solid-phase Extraction and Gas Chromatography. J. Appl. Sci. 10 (2010) 1987-1990.

8. Y.M. Lee, J.E. Lee, W. Choe, T. Kim, J.Y. Lee, Y. Kho, K. Choi, K.D. Zoh, Distribution of phthalate esters in air, water, sediments, and fish in the Asan Lake of Korea. Environ. Int. 126(2019) 635-643.

9. W. Brueller, N. Inreiter, T. Boegl, M. Rubasch, S. Saner, F. Humer, W. Moche, A. Schuhmann, W. Hartl, C. Brezinka, L. Wildt, F. Allerberger, Occurrence of chemicals with known or suspected endocrine disrupting activity in drinking water, groundwater and surface water, Austria 2017/2018. Die Bodenkultur: Journal of Land Management, Food and Environment. 69(2018) 155-173.

10. P. Gimeno, A.F. Maggio, C. Bousquet, A. Quoirez, C. Civade, P.A. Bonnet, Analytical method for the identification and assay of 12 phthalates in cosmetic products: Application of the ISO 12787 international standard Cosmetics- Analytical methods-Validation

criteria for analytical results using chromatographic techniques. J. Chromatogr. A. 1253(2012) 144-153.

11. M.F. Zaater, Y.R. Tahboub, A.N. Al Sayyed, Determination of Phthalates in Jordanian Bottled Water using GC-MS and HPLC-UV: Environmental Study. J. Chromatogr. Sci. 52(2014) 444-452.

12. J. Annamalai, V. Namasivayam, Determination of effect of pH and storage temperature on leaching of phthalate esters from plastic containers by ultrasound-assisted dispersive liquid–liquid micro-extraction. J. Food Meas. Charact. 11(2017) 2222-2232.

13. S.H. Jeon, Y.P. Kim, Y. Kho, J.H. Shin, W.H. Ji, Y.G. Ahn, Development and Validation of Gas Chromatography-Triple Quadrupole Mass Spectrometric Method for Quantitative Determination of Regulated Plasticizers in Medical Infusion Sets. J. Anal. Methods Chem. 9470254 (2018) 1-9.

14. M.S. Qureshi, J. Fischer, J. Barek, Sirajuddin, M.I. Bhangera, Voltammetric Determination of Aliphatic Phthalate Esters at a Hanging Mercury Drop Minielectrode and a Meniscus Modified Silver Solid Amalgam Electrode. Electroanalysis. 22(2010) 1957-1962.

15. H.B. Noh, N.G. Gurudatt, M.S. Won, Y.B. Shim, Analysis of Phthalate Esters in Mammalian Cell Culture Using a Microfluidic Channel Coupled with an Electrochemical Sensor. Anal. Chem. 21(2015) 7069-7077.

16. X. Zhao, X. Ju, S. Qiu, W. Hu, L. Yang, J. Zhang, Fast and Sensitive Detection of Diisononyl Phthalate in Liquor Sample by Molecularly Imprinted Polymer Based

Electrochemical Sensor. Russ. J. Electrochem. 54(2018) 636-643.

17. A.I. Zia, A.R. Mohd Syaifudin, S.C. Mukhopadhyay, P.L. Yu, H. Al-Bahadly, C.P. Gooneratne, J. Kosel, T.S. Liao, Electrochemical impedance spectroscopy based MEMS sensors for phthalates detection in water and juices. J. Phys. Conf. Ser. 439(2013) 01202.

18. J. Annamalai, N. Vasudevan, Enhanced Biodegradation of an Endocrine Disrupting Micro-pollutant: Di (2-ethylhexyl) phthalate using Biogenic Self-assembled Monolayer of Silver Nanoparticles. Sci. Total Environ. 719(2020) 1-11.

19. A. Jayshree, N. Vasudevan, Bacterial enzyme based spectrophotometric determination of phthalate esters in drinking water stored in PET bottles. J. Food Measur. Charact. 13(2019) 2190-2202.

20. S.H. Park, J. Kim, W.E. Lee, D.J. Byun, M.H. Kim, One-Step Synthesis of Hollow Dimpled Polystyrene Microparticles by Dispersion Polymerization. Langmuir. 33(2017) 2275-2282.

21. X. Feng, C. Mao, G. Yang, W. Hou, J. Zhu, Polyaniline/Au Composite Hollow Spheres: Synthesis, Characterization, and Application to the Detection of Dopamine. Langmuir. 22(2006) 4384-4389.

22. A.A. Muataz, F. Ahmadun, C. Guan, E. Mahdi, A. Rinaldi, Effect of reaction temperature on the production of carbon nanotube. Nano. 1(2006) 251-257.

23. A. Khan, A. Rashid, R. Younas, R. Chong, A chemical reduction approach to the synthesis of copper nanoparticles. Int Nano Lett. 6(2016) 21-26.

24. Y. Zhu, Y. Cao, X. Sun, X. Wang, Amperometric immunosensor for carbofuran detection

based on MWCNTs/GS-PEI-Au and AuNPs-antibody conjugate. Sensors. 13(2013), 5286-5301.

25. M. Saeed, Sirajuddin, A. Niaz, A. Shah, H.I. Afridia, A. Raufa, Fast voltammetric assay of water soluble phthalates in bottled and coolers water. Anal. Methods. 2(2010) 844-850.

26. M.A. Atieh, O.Y. Bakather, B. Al-Tawbini, A.A. Bukhari, F.A. Abuilaiwi, M.B. Fettouhi, Effect of Carboxylic Functional Group Functionalized on Carbon Nanotubes Surface on the Removal of Lead from Water. Bioinorg. Chem. Appl. 603978 (2010) 9.

27. M.A.C. Mazzeu, L.K. Faria, A.M. Cardoso, A.M. Gama, M.R. Baldan, E.S. Goncalves, Structural and Morphological Characteristics of Polyaniline Synthesized in Pilot Scale. J. Aerosp. Technol. Manag. 9(2017) 1-7.

28. A.N. Jarad, K. Ibrahim, N.M. Ahmed, Synthesis and characterization thin films of conductive polymer (PANI) for optoelectronic device application. AIP Conf. Proc. 1733(2016) 020020.

29. X. Li, L. Tao, Z. Chen, H. Fang, X. Li, X. Wan, J.B. Xu, H. Zhu, Graphene and related two-dimensional materials: Structure-property relationships for electronics and optoelectronics. Appl. Phys. Rev. 4(2017) 021306.

30. F. Jaouen, J. Herranz, M. Lefevre, J.P. Dodelet, U.I. Kramm, I. Herrmann, P. Bogdanoff, J. Maruyama, T. Nagaoka, A. Garsuch, J.R. Dahn, T. Olson, S. Pylypenko, P. Atanassov, E.A. Ustinov, Cross-laboratory experimental study of non-noble-metal electrocatalysts for the oxygen reduction reaction', ACS Applied Material Interfaces. 1(2009) 1623-1639.

31. G. Wu, C.M. Johnston, N.H. Mack, K. Artyushkova, M. Ferrandon, M. Nelson, J.S. Lezama-Pacheco, S.D. Conradson, K.L. More, D.J. Myers, P. Zelenav, Synthesis structure performance correlation for polyaniline-Me-C non-precious metal cathode catalysts for oxygen reduction in fuel cells. J. Mater. Chem. 21 (2011). 11392-11405

32. A. Morozan, P. Jegou, B. Jousselme, S. Palacin, Electrochemical performance of annealed cobalt–benzotriazole/CNTs catalysts towards the oxygen reduction reaction. Phys. Chem. Chem. Phys. 13(2011) 1600-21607.

33. Y. Mosqueda, E. Perez-Cappe, J. Arana, E. Longo, A. Ries, M. Cilense, P.A.P. Nascente, P. Aranda, E. Ruiz-Hitzky, Preparation and characterization of $LiNi_{0.8}Co_{0.2}O_2$/PANI microcomposite electrode materials under assisted ultrasonic irradiation. J. Solid State Chem. 179(2006) 308-314.

34. P.R. Somania, R. Marimuthu, A.B. Mandale, Synthesis, characterization and charge transport mechanism of conducting polyaniline / V2O5 composites. Polymer. 42(2001) 2991-3001.

35. Y. Zou, C. Xiang, L.X. Sun, F. Xu, Glucose biosensor based on electrodeposition of platinum nanoparticles onto carbon nanotubes and immobilizing enzyme with chitosan-SiO2 sol-gel. Biosens. Bioelectron. 23(2008) 1010-1016.

36. X. Kang, Z. Mai, X. Zou, P. Cai, J. Mo, A novel glucose biosensor based on immobilization of glucose oxidase in chitosan on a glassy carbon electrode modified with gold–platinum alloy nanoparticles/multiwall carbon nanotubes. Anal. Biochem. 369(2007) 71-79.

37. J. Lin, C. He, Y. Zhao, S. Zhang, One-Step synthesis of silver nanoparticles/ carbon nanotube/chotisan film and it application in glucose biosensor. Sens. Actuators B Chem. 137(2009) 768-777.

38. F.N. Crespilho, R.M. Iost, S.A. Travain, O.N. Oliveira Jr, V. Zucolotto, Enzyme immobilization on Ag nanoparticles/polyaniline nanocomposites. Biosens. Bioelectron. 29(2009) 3073-3077.

39. K. Zhang, G. Fan, R. Hu, G. Li, Enhanced dibutyl phthalate sensing performance of a Quartz crystal microbalance coated with Au-decorated ZnO porous microspheres. Sensors. 15(2015) 21153-21168.

40. A.I. Zia, S.C. Mukapadhyay, P.K. Yu, I.H. Al-Bahadly, C.P. Gooneratne, J. Kosel, Rapid and molecular selective electrochemical sensing of phthalates in aqueous solution. Biosens. Bioelectron. 67(2015) 342-349.

Figures

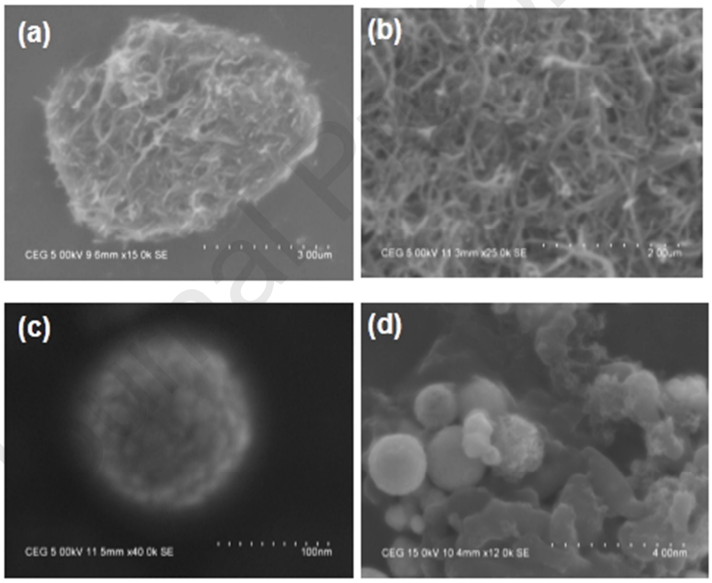

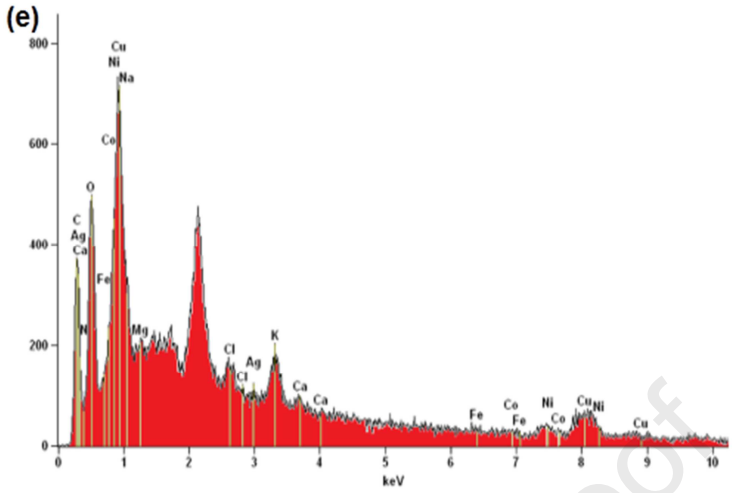

Figure 1. (a) PANI hollow sphere, (b) f-MWCNT, (c) CuNP, (d) Nanocomposite material: PANI/CNT/CuNP, (e) EDAX

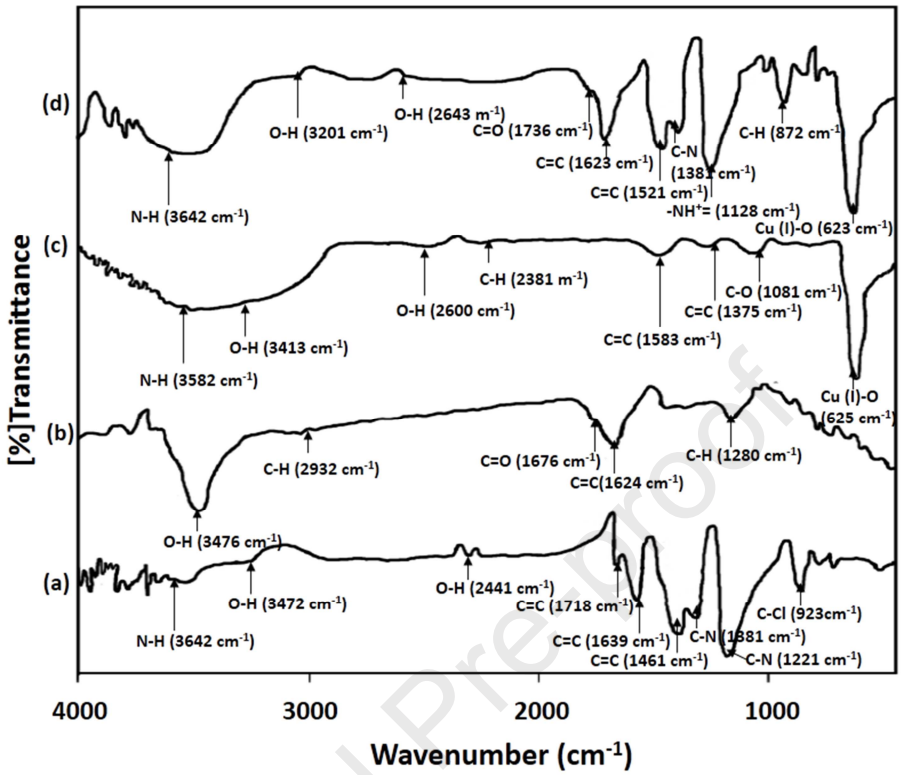

Figure 2. FTIR Spectrum of (a) PANI, (b) f-MWCNT, (c) CuNP, (d) Nanocomposite material: PANI/CNT/CuNP

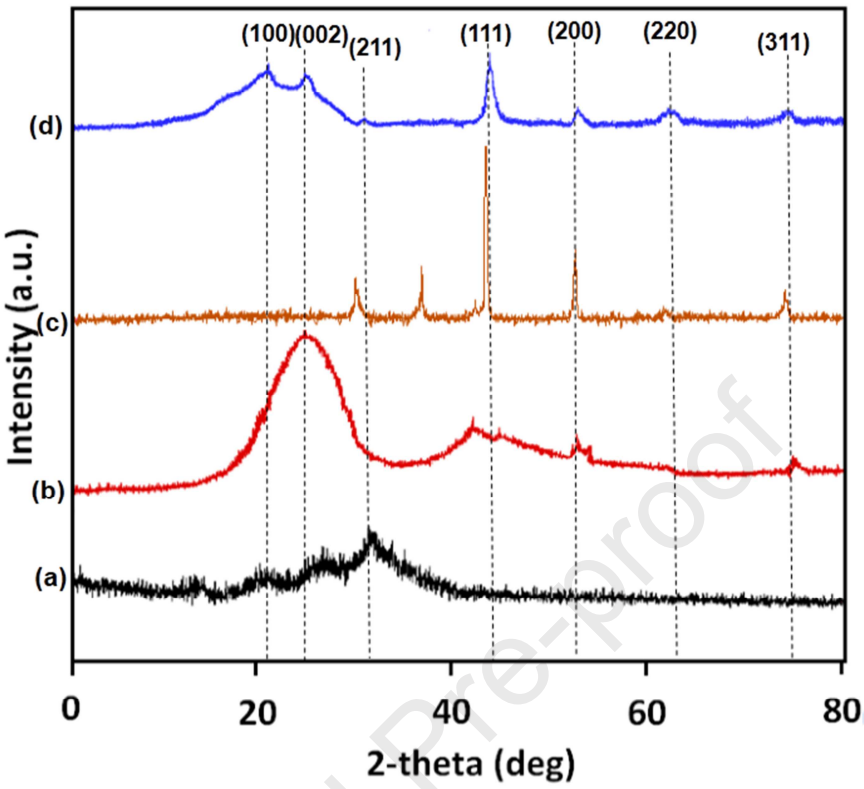

Figure 3. XRD Analysis of (a) PANI, (b) f-MWCNT, (c) CuNP, (d) Nanocomposite material: PANI/CNT/CuNP

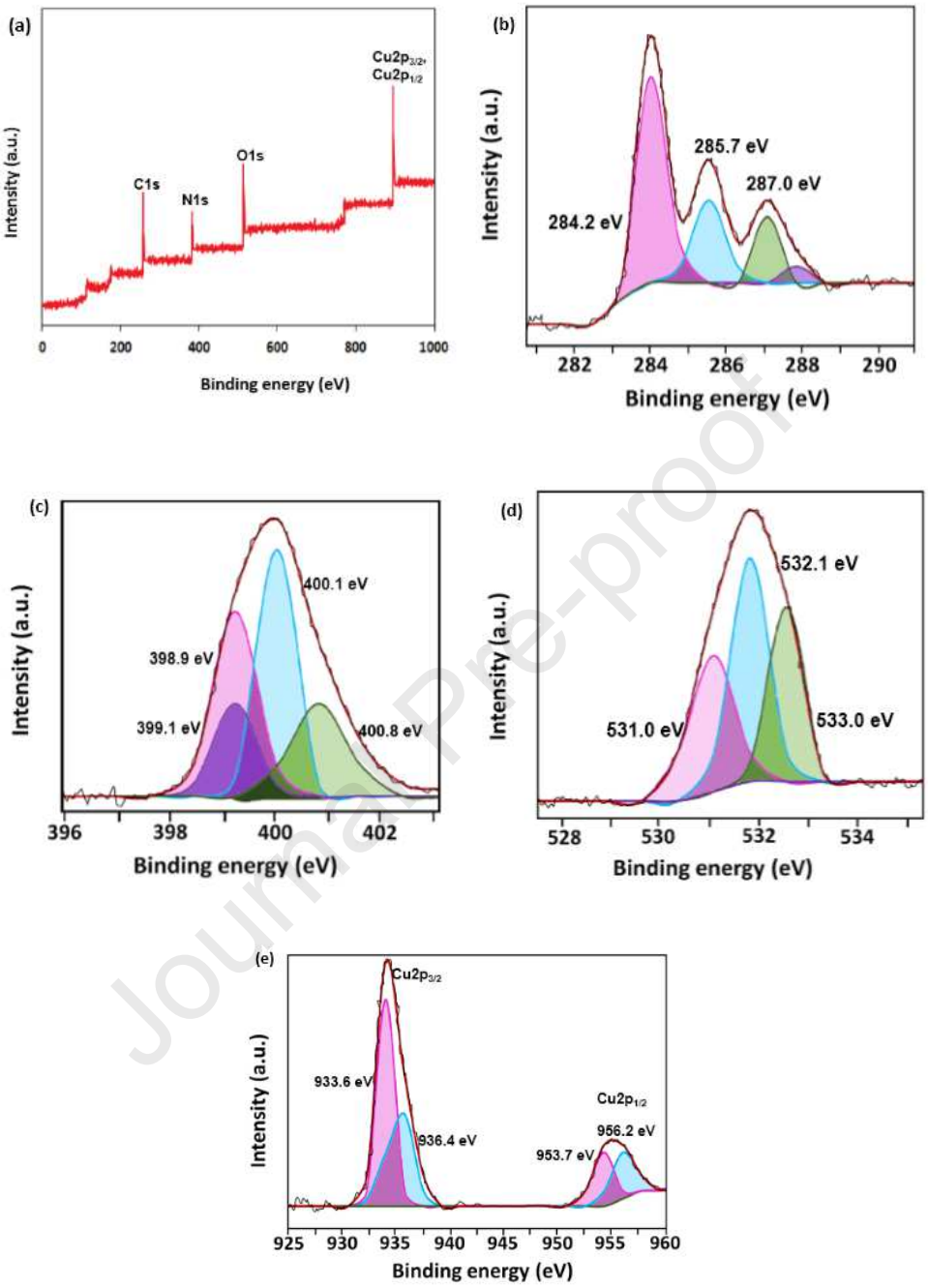

Figure 4. XPS analysis of Nano-composite material: PANI/CNT/CuNP. (a) Survey spectrum and Deconvoluted peaks of (b) Carbon (C1s), (c) Nitrogen (N1s), (d) Oxygen (O1s), (e) Copper ($Cu2p_{3/2}$ and $Cu2p_{1/2}$)

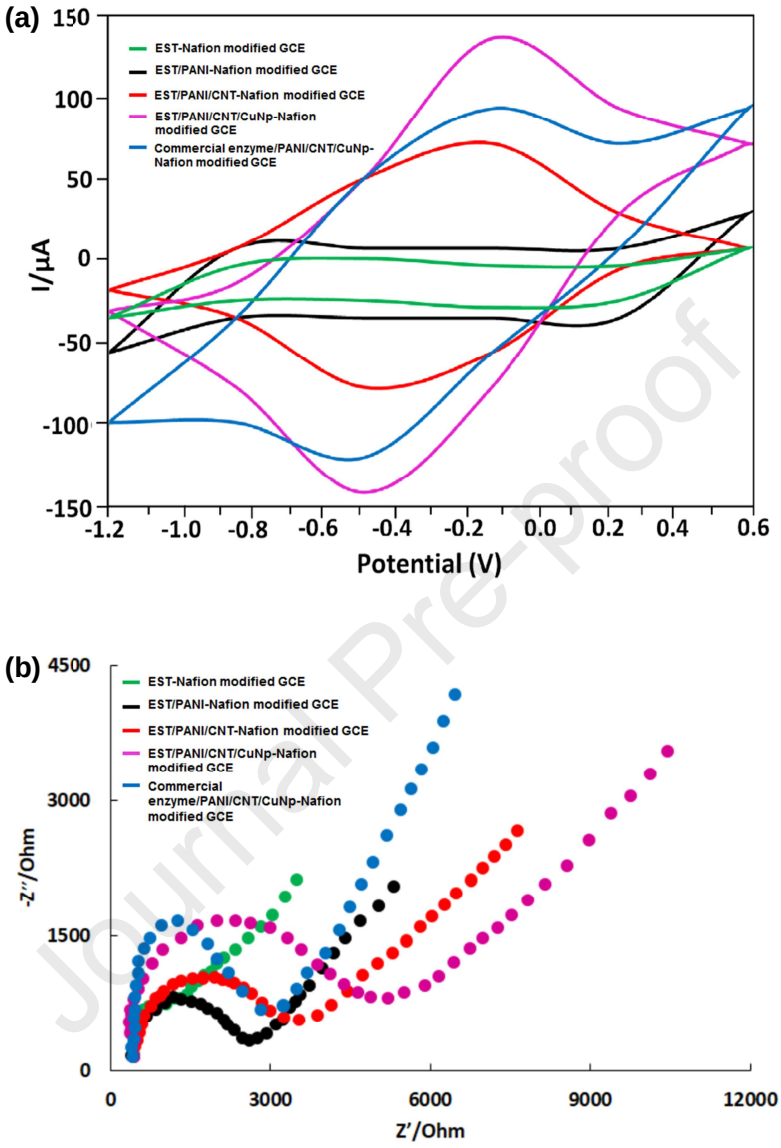

Figure 5. CV Curves and EIS (Nyquist plot) of surface modified Electrodes with PANI, CNTs, CuNPs and EST enzyme

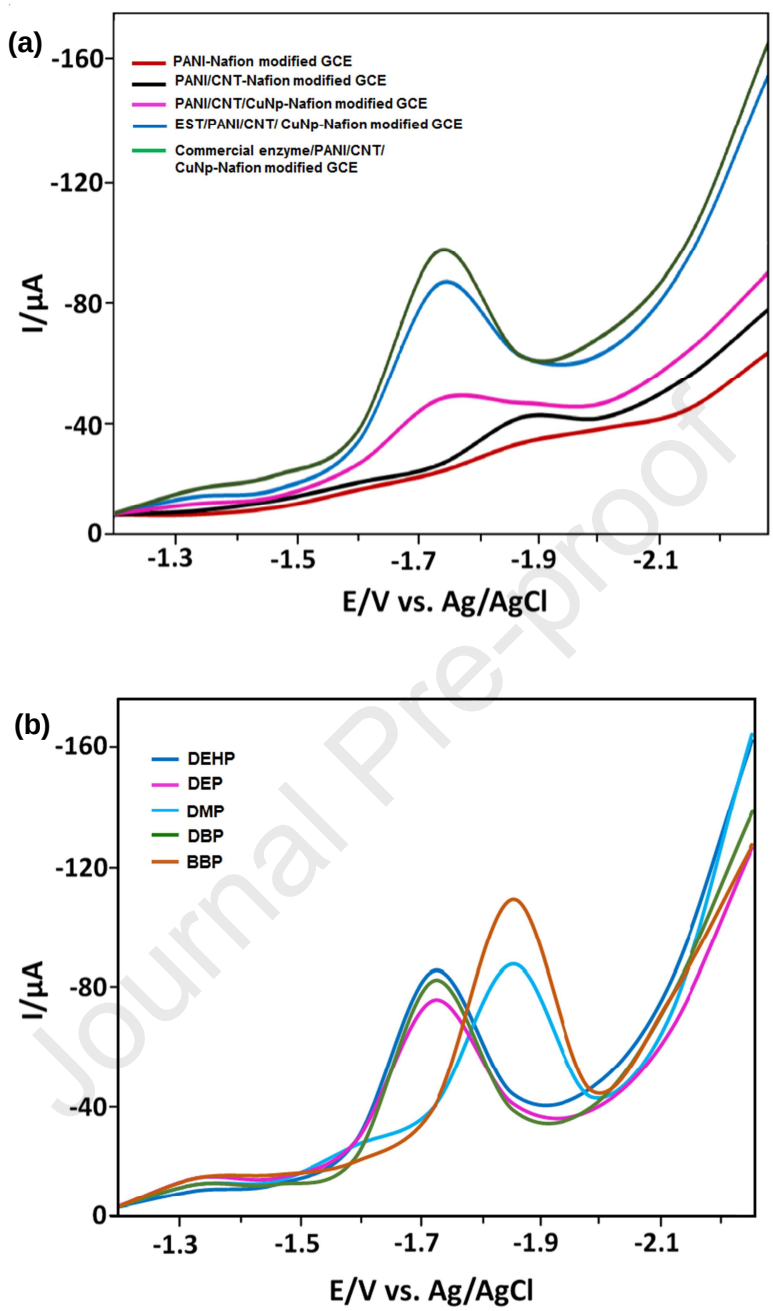

Figure 6. LSV analysis of @EST/PANI/CNT/CuNP-NF modified GCE (a) response to varied electrode components at 1x 10^{-5} mmol L^{-1} DEHP concentration, (b) response to varied PEs at 1x 10^{-5} mmol L^{-1} concentration

Table 1. Calibration parameter for the determination PEs @EST/PANI/CNT/CuNP-NF modified GCE

Phthalate esters	Concentration (mmol L^{-1})	Slope (µA nmol $L^{-1})^{-1}$	Intercept (µA)	Correlation coefficient	LoD (nmol L^{-1})	LoQ (nmol L^{-1})
DEHP	(2-10) x 10^{-5}	-72.1	5.5	0.9947	-	-
	(2-10) x 10^{-6}	-79.0	3.8	0.9950	-	-
	(2-10) x 10^{-7}	-77.4	-4.9	0.9954	0.06	0.2
DEP	(2-10) x 10^{-5}	-73.5	5.3	0.9942	-	-
	(2-10) x 10^{-6}	-77.0	3.2	0.9961	-	-
	(2-10) x 10^{-7}	-84.0	1.0	0.9987	0.08	0.2
DMP	(2-10) x 10^{-5}	-69.8	22.9	0.9979	-	-
	(2-10) x 10^{-6}	-72.7	18.0	0.9963	-	-
	(2-10) x 10^{-7}	-73.1	12.6	0.9933	0.03	0.1
DBP	(2-10) x 10^{-5}	-84.6	13.4	0.9964	-	-
	(2-10) x 10^{-6}	-80.9	12.4	0.9958	-	-
	(2-10) x 10^{-7}	-90.2	7.5	0.9954	0.04	0.1
BBP	(2-10) x 10^{-5}	-76.3	23.9	0.9910	-	-
	(2-10) x 10^{-6}	-79.8	18.8	0.9903	-	-
	(2-10) x 10^{-7}	-75.4	10.0	0.9997	0.04	0.1

Table 2. Intra-day and Inter-day precision of PEs @EST/PANI/CNT/CuNP-NF modified GCE

Analyte	Spiked volume (x mmol L^{-1})	Intra-day			Inter-day		
		Quantified volume (x mmol L^{-1})	RSD %	Accu racy %	Quantified volume (x mmol L^{-1})	RSD %	Accu -racy %
DEHP	1	1.006 ± 0.001	0.1	100	1.001 ± 0.003	0.3	100
DEP	1	1.003 ± 0.006	0.6	99	1.009 ± 0.01	1.2	100
DMP	1	1.003 ± 0.001	0.0	99	0.999 ± 0.006	0.6	99
DBP	1	0.999 ± 0.004	0.4	98	0.995 ± 0.024	2.4	99
BBP	1	0.985 ± 0.037	3.7	98	0.999 ± 0.01	1.0	99
DEHP+DEP	2	1.961 ± 0.053	2.7	98	1.94 ± 0.049	2.5	97
DEHP+DMP	2	1.96 ± 0.058	3.0	98	1.998 ± 0.002	1.0	100
DEHP+DBP	2	1.967 ± 0.059	3.0	98	1.97 ± 0.058	2.9	98
DEHP+BBP	2	1.988 ± 0.113	0.5	99	2.002 ± 0.002	0.1	100
DEP+DMP	2	1.931 ± 0.062	3.2	96	1.977 ± 0.030	1.5	98
DMP+DBP	2	1.999 ± 0.001	0.08	99	2.008 ± 0.007	0.3	100
DBP+BBP	2	1.998 ± 0.004	0.2	100	1.973 ± 0.04	2.3	98
DEHP+DEP+DMP	3	2.993 ± 0.011	0.3	100	3.0 ±0.007	0.2	100
DEHP+DEP+DMP +DBP	4	4.008 ± 0.007	0.1	100	3.97 ± 0.06	1.5	99
DEHP+DEP+DMP +DBP+BBP	5	5.003 ± 0.007	0.1	100	4.966 ± 0.058	1.1	99

Table 3. Efficiency of EST/PANI/CNT/CuNP-NF modified GCE Vs existing Electro-chemical methods in PE detection

PE source and quantification	Mode of detection	Detection limit (LoD)	Reference
Drinking water, 0.24- 0.52 µmol L^{-1}	Enzyme and nanocomposite material based NF modified GCE	DEHP, DEP, DMP, DBP, BBP: 0.06, 0.08, 0.03, 0.04, 0.04 nmol L^{-1}	Present study
Soft drink, 4.10- 12.65 µmol L^{-1}	Enzyme and nanocomposite material based NF modified GCE	DEHP, DEP, DMP, DBP, BBP: 0.06, 0.08, 0.03, 0.04, 0.04 nmol L^{-1}	Present study
Beverages, 0.22- 1.82 µmol L^{-1}	Enzyme and nanocomposite material based NF modified GCE	DEHP, DEP, DMP, DBP, BBP: 0.06, 0.08, 0.03, 0.04, 0.04 nmol L^{-1}	Present study
Lake water, 3.146 µmol L^{-1}	Enzyme and nanocomposite material based NF modified GCE	DEHP, DEP, DMP, DBP, BBP: 0.06, 0.08, 0.03, 0.04, 0.04 nmol L^{-1}	Present study
Liquor samples, 5.0-20.0 mM	Molecularly imprinted polymer based GCE	DINP: 27 nM	[16]
Manicure and PVC products, 0.15 nM-10.0 µM	Microfluidic channel coupled with an electrochemical sensor	PEs: and ~12.5-35.2 pM	[15]
Gas particulates, 20 ppb-2 ppm	Quartz crystal microbalance coated with Au decorated ZnO porous microspheres	DBP: <1.0 ppb	[39]
DEHP in deionized MilliQ water	EIS technique incorporating a novel interdigital capacitive sensor	Linear range of response between 1-100 µg mL^{-1}	[40]
Water and juices, 20 ppm	EIS based on micro electro-mechanical system	Detection range, DEHP: 0.002- 2.0 ppm	[17]
Water stored in PVC coolers and plastic bottles, 0.728 µmol L^{-1}	Square wave voltammetric analysis using GCE	Water soluble PEs (DMP, DEP, DBP, DPP): 0.47 µmol L^{-1}	[25]

Non-aqueous methanolic extract, 1.0-3.0 x 10^{-5} M	1. Solid phase extraction combined with hanging mercury drop minielectrode detection (HMDmE) 2. Solid phase extraction combined with modified silver solid amalgam electrode detection (AgSAE)	1. HMDmE DEP: 0.3 µM DBP: 0.3 µM DDP: 0.5 µM DAP: 0.3 µM 2. AgSAE DEP: 3.0 µM DBP: 2.0 µM DDP: 4.0 µM DAP: 4.0 µM	[14]

Note: DINP: diisononyl phthalate; DDP- didecyl phthalate; DAP: dially phthalate

Highlights

- Phthalate esters, modulator in PET bottle manufacturing and a critical environmental pollutant are endocrine disruptors
- Detection of phthalates: nano and micro level toxicant via., conventional methods is expensive
- This is first report on esterase enzyme based electrochemical detection of phthalate esters
- Limit of detection for phthalate esters ranges between 0.03-0.08 nmol L^{-1}
- Enzyme and nanocomposite modified glassy carbon electrode tends to be simple and cost -effective

Declaration of interests

☒ The authors declare that they have no known competing financial interests or personal relationships that could have appeared to influence the work reported in this paper.

☐The authors declare the following financial interests/personal relationships which may be considered as potential competing interests: